Biochimica et Biophysica Acta 1837 (2014) 1165–1177

Contents lists available at ScienceDirect

Biochimica et Biophysica Acta

journal homepage: www.elsevier.com/locate/bbabio

Proton pumping in cytochrome c oxidase: Energetic requirements and the role of two proton channels ☆

Margareta R.A. Blomberg *, Per E.M. Siegbahn

Department of Organic Chemistry, Arrhenius Laboratory, Stockholm University, SE-106 91, Stockholm, Sweden

ARTICLE INFO

Article history:
Received 31 October 2013
Received in revised form 2 January 2014
Accepted 6 January 2014
Available online 11 January 2014

Keywords:
Cytochrome c oxidase
Proton pumping
Density functional theory
Energy profiles

ABSTRACT

Cytochrome c oxidase is a superfamily of membrane bound enzymes catalyzing the exergonic reduction of molecular oxygen to water, producing an electrochemical gradient across the membrane. The gradient is formed both by the electrogenic chemistry, taking electrons and protons from opposite sides of the membrane, and by proton pumping across the entire membrane. In the most efficient subfamily, the A-family of oxidases, one proton is pumped in each reduction step, which is surprising considering the fact that two of the reduction steps most likely are only weakly exergonic. Based on a combination of quantum chemical calculations and experimental information, it is here shown that from both a thermodynamic and a kinetic point of view, it should be possible to pump one proton per electron also with such an uneven distribution of the free energy release over the reduction steps, at least up to half the maximum gradient. A previously suggested pumping mechanism is developed further to suggest a reason for the use of two proton transfer channels in the A-family. Since the rate of proton transfer to the binuclear center through the D-channel is redox dependent, it might become too slow for the steps with low exergonicity. Therefore, a second channel, the K-channel, where the rate is redox-independent is needed. A redox-dependent leakage possibility is also suggested, which might be important for efficient energy conservation at a high gradient. A mechanism for the variation in proton pumping stoichiometry over the different subfamilies of cytochrome oxidase is also suggested. This article is part of a Special Issue entitled: 18th European Bioenergetic Conference.

1. Introduction

In aerobic respiration, molecular oxygen is reduced to water, a very exergonic reaction where a substantial part of the energy is conserved as an electrochemical gradient over the mitochondrial or bacterial membrane. The membrane gradient is used by ATP synthase to transform ADP to ATP, the energy currency of the cell. The terminal enzyme in the respiratory chain is often a member of the heme-copper oxidase family, also referred to as cytochrome c oxidase (CcO) since the electron donor is cytochrome c. The basic process for building up an electrochemical gradient is to transport charges from one side of the membrane to the other. In the heme-copper oxidases the charge transport occurs in two different ways. First, the chemistry of the O_2 reduction to water occurs by taking up the electrons and the protons from opposite sides of the membrane, giving a so called electrogenic reaction. The electron donor, cytochrome c is located on the P-side of the membrane (intermembrane space or periplasm), and by taking up the protons from the other side, the N-side (matrix or cytoplasm), each electron- and proton-pair used in the chemistry corresponds to the movement of one positive charge from the N-side to the P-side, see Fig. 1. Secondly, coupled to the exergonic chemistry, an active transport of protons from the N-side of the membrane all the way to the P-side, increases the efficiency of the energy conservation. The second process is referred to as proton pumping. The heme-copper oxidases are the only oxygen reductases known to pump protons [1,2]. The reduction of one O_2 molecule can be written as follows, where n is the number of protons pumped per electron (see further below):

$$O_2 + 4(1+n)H_N^+ + 4e_P^- \rightarrow 2H_2O \;\; 4nH_P^+ \qquad (1)$$

Both the electrogenic chemistry and the proton pumping require proton motion against the gradient. This implies the existence of a set of kinetic barriers, gating the protons to move in the right direction. In particular, due to the presence of proton pumping, some barrier heights must change during the reaction, to prevent proton uptake from the P-side at certain stages of the reaction, still allowing protons to be pumped to the P-side at other stages. A detailed description of how reaction (1), including gating, occurs is referred to as a proton pumping mechanism. To find those details is the goal of a large part of current research in bioenergetics, see for example ref. [3]. Significant knowledge and insight in these processes have already been gained [4–11], but some important unresolved questions still remain, which motivates the present study. The heme-copper oxidases have been divided into subfamilies [12], differing among other things in the exact form of the redox-active

☆ This article is part of a Special Issue entitled: 18th European Bioenergetic Conference.

* Corresponding author. Tel.: +46 8 16 26 16.
E-mail address: mb@organ.su.se (M.R.A. Blomberg).

0005-2728/$ – see front matter © 2014 Elsevier B.V. All rights reserved.
http://dx.doi.org/10.1016/j.bbabio.2014.01.002

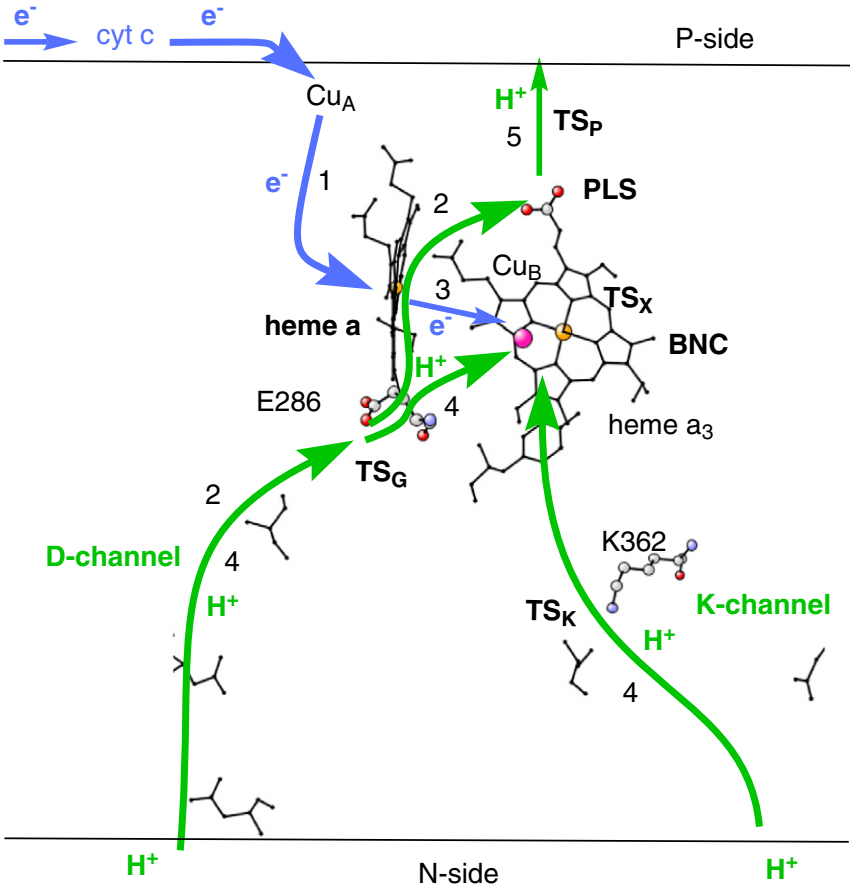

Fig. 1. Overview of electron and proton transfer in CcO (A-family). The numbers refer to the elementary steps in the proton pumping mechanism discussed in Section 3.2. The D-channel is known to be used for all protons pumped and for two of the protons to the BNC. The K-channel is only used for the remaining two protons to the BNC, see further in the text.

cofactors. Most knowledge has been gained for cytochrome c oxidases belonging to the largest family, the so called A-family, which is also the main target for the present investigation. One difference between the A-family and the other oxidase families (B and C) is the stoichiometry of the proton pumping, i.e. the value of n in Eq. (1). A-family oxidases have been found to pump four protons per oxygen molecule, i.e. n is equal to one (one proton pumped per electron), while oxidases from the B- and C-families have a lower value of n (probably close to 0.5) [2]. Another difference is that the A-family oxidases have two channels for proton uptake, the D- and the K-channels, see Fig. 1, while the B- and C-families only have one, often referred to as the K-channel analog since it is located in the same place as the K-channel in the A-family [2].

One of the most important unresolved questions for the cytochrome c oxidases concerns the uneven distribution of the free energy released in the four reduction steps in Eq. (1) [10,13,14]. The active site where the chemistry of the transformation of molecular oxygen to water occurs is a binuclear center (BNC) consisting of a high spin heme group (heme a_3 in A-family oxidases) and a copper complex (Cu_B) with a tyrosine residue cross-linked to one of its histidine ligands. The O_2 molecule binds reversibly to the reduced BNC, **R** (Fe(II) and Cu(I)), forming intermediate **A**, and in the next step the O–O bond is cleaved, forming intermediate $\mathbf{P}_M$. In the **R** to $\mathbf{P}_M$ reaction steps, the active site redox centers provide all four electrons to the oxygens: Fe(II) is oxidized to Fe(IV), Cu(I) is oxidized to Cu(II) and the tyrosine is oxidized to a neutral radical, see the scheme in Fig. 2. To complete the catalytic cycle of Eq. (1) and return to the reduced BNC, **R**, four electrons and four protons (to complete the water formation) has to be taken up by the enzyme, which occurs in four separate reduction steps. Based on experimental mid-point potentials it was early noted that the free energy release seems to be much larger in the first two reduction steps after the O–O bond cleavage, $\mathbf{P}_M$ to **O** (often referred to as the oxidative part of the catalytic cycle) than in the reduction steps **O** to **R** (referred to as the reductive part) [13]. Later, quantum chemical calculations on the catalytic cycle have given the same picture, with large exergonicities in the first two reduction steps after the O–O bond cleavage, and very small exergonicities in the other two reduction steps [15–17]. It has therefore been a point of major concern, that even if the total free energy released in the O_2 reduction is more than enough for pumping four protons across the membrane, the free energies for two of the steps, **O** to **E**, and **E** to **R**, do not seem to be large enough to afford proton pumping, at least not with a significant gradient across the membrane [10,14,18,19]. At an early stage this situation even led to the suggestion that all four protons were pumped in the first two reduction steps after O–O bond cleavage, i.e. two protons pumped per electron in these steps, and no proton pumping in the other two reduction steps [20]. It was later shown experimentally that there is actually one proton

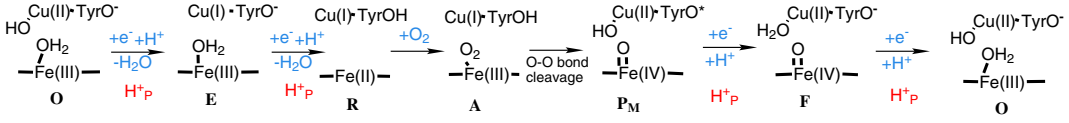

Fig. 2. Catalytic cycle of CcO starting from the oxidized state O. The notation H^+_P corresponds to pumped protons.

pumped per electron in all four reduction steps [18,21,22]. To explain how this can occur in spite of the small energy release in two of the reduction steps has become one of the most important challenges in the field. It has been suggested that part of the free energy from the $\mathbf{P}_M$ to **O** reduction steps somehow must be temporarily stored by the enzyme, to be used in the next two steps, making them more exergonic and thereby making proton pumping possible also in those steps [14,18,21]. It has furthermore been suggested that there exist two different forms of the **O** and **E** states, where one of the forms is activated by the energy saved [10,18,19]. However, so far no spectroscopic evidence for two different forms of these intermediates has been found [23] and no other evidence has been presented for how this temporary energy storage might occur. Based on both experiments and calculations, the presently most likely situation is that there is a quite small driving force in two of the four reduction steps, and that scenario is therefore here taken as the starting point. Using the calculated energy profile for the entire catalytic cycle, having a much larger exergonicity in the first two reductions steps after O – O bond cleavage compared to the other two reduction steps, the kinetic and thermodynamic requirements for proton pumping are investigated.

The low exergonicity in two of the reduction steps makes it particularly difficult to pump protons when a high gradient is present. The uneven distribution of the free energy released in the different reduction steps brings up another important question, which concerns possible mechanisms for decreasing the stoichiometry of proton pumping when the gradient increases. Experimental information has been interpreted to indicate that at higher values for the gradient across the membrane, the stoichiometry of the proton pumping actually goes down, i.e. on the average less than four protons per oxygen molecule are pumped for the A-family oxidases [24]. Recent interpretations of the experimental data indicate that, also at a significant gradient the pumping stoichiometry is fairly high (3.2–3.7 protons) [25,26]. Still, it should be of interest to investigate mechanisms for decreasing proton pumping at higher gradients, and in particular, if the decrease can occur in an efficient way, i.e. the uncoupling of proton pumping from the chemistry should occur *only* for the reduction steps with the lower exergonicity.

There exist many different suggestions for the pumping mechanism in CcO, and most of them agree on the general sequence of events: Electron transfer leads to uptake of a proton from the N-side of the membrane to a pump loading site (PLS), followed by uptake of a second proton from the N-side to the active site (the BNC) for the chemistry, see Fig. 1. Finally the electrostatic repulsion between the two protons leads to release of the proton at the pump loading site to the P-side [27]. Possible mechanisms for uncoupling of proton pumping at high membrane gradient have not been much discussed. It is here suggested that it is unlikely that such an uncoupling would occur by preventing the proton uptake to the pump loading site, since this would require a shift to a distinctly different reaction mechanism when the uncoupling occurs. Assuming a pump mechanism like the one suggested on the basis of a kinetic experiment on one reduction step [11,28–31], uncoupling of proton pumping is more likely the result of a leakage of the proton in the pump loading site, either back to the N-side or to the BNC. It is trivial to suggest that such a leakage occurs because some barrier for a desired reaction step, due to the gradient has become higher than a leakage barrier. However, since it would be very inefficient for the enzyme to allow the pump-protons to leak in all reduction steps, including those with high exergonicity where leakage is not required, an efficient leakage mechanism should be dependent on the exergonicity of the specific reduction step, which is not trivial to accomplish. In this context, it is interesting to recall the experimentally observed shift from using the D-channel for uptake of the chemical protons to using the K-channel in the two reduction steps from **O** to **R**, i.e. in the reduction steps with low exergonicity [32–34]. In the present contribution a role of the two proton channels is suggested, which also allows for a redox dependent proton leakage mechanism.

Another problem related to the questions discussed above, concerns the variation in proton pumping stoichiometry between the different oxidase families. At least for the B-family oxidases it seems to be established that two protons are pumped across the membrane per oxygen molecule, i.e. there is a factor of two in proton pumping efficiency between the A- and the B-family oxidases [2]. The reason for this difference between the A- and the B-families is not known, but it has been suggested to be caused by the presence of only one proton channel in the B-family, which in turn might be an adaptation to the low concentration of O_2 in the environment [2,35,36]. The mechanism for the variation in proton pumping is not understood, but it has been suggested that the lower number of protons pumped in the B-family is achieved by uptake and release of the pumped proton in different steps, i.e. a proton is taken up to the PLS in one reduction step and released to the P-side in the next reduction step [35]. This scheme would lead to one proton pumped in the first two reduction steps after the O – O bond cleavage, from $\mathbf{P}_M$ to **O**, and one proton pumped in the two reduction steps from **O** to **R**, i.e. a total of two pumped protons per oxygen molecule. Again assuming the uneven distribution of the free energy released in the different reduction steps, a different scenario is discussed here, namely that for the B-family oxidases only the two most exergonic steps pump protons, i.e. only in the first two reduction steps after the O – O bond cleavage. The general properties of the proton pumping mechanism suggested in the present study can be used to suggest a mechanism for the lower pumping stoichiometry of the B-family oxidases.

The basic purpose of the present study is to investigate the consequences of the fact that the free energy released in CcO seems to be quite unevenly distributed between the reduction steps, as indicated by all present experimental and computational information. For this purpose an energy profile describing the O_2 reduction reaction as depicted in the scheme in Fig. 2 is needed. Accurate relative energies of the reduction steps cannot be obtained from experimental values, since it is not possible to determine the actual reduction potentials of the particular BNC intermediates involved in each individual reduction step. Therefore, quantum chemical calculations on a model of the active site in an A-family cytochrome c oxidase have been used to construct an energy profile of the catalytic cycle. To calculate reaction energies involving changes in the oxidation state of transition metals is a difficult task. However, the methodology used here can be considered as the best one available for this type of system, and it has been shown to provide reliable results for the opposite reaction, water oxidation, in photosystem II [37]. Furthermore, the results obtained from the calculations agree well with the general expectations from available experimental values. The barriers needed to complete the energy profile can rather safely be deduced from experimental rate measurements. Thus, the energy profile obtained in this way is used to analyze kinetic and thermodynamic requirements for proton pumping in all reduction steps. It should be stressed that the accuracy of the model calculations for the reduction potentials is still not high enough to answer the questions above in an unequivocal way. The calculated energetics should therefore be considered to give a qualitative picture.

A thorough analysis of the conditions for proton pumping in all reduction steps, also requires that the previously suggested mechanism for proton pumping [11,29,30] is developed further. For this purpose detailed energy profiles for the individual reduction steps are needed. Also for these energy profiles results from experimental rate measurements play an important role. To incorporate gating in the proton pumping mechanism, these energy profiles must include forbidden reaction paths, which can be derived only from theory. The energy profiles obtained in this way can be used to analyze the different gating situations and also to explore the differences between the reduction steps. The present procedure, combining experimental and theoretical energy values, might seem somewhat arbitrary. However, when the detailed diagrams are finally constructed, the actual span of values leading to proton pumping is quite limited. Changing a value by only a few kcal/mol can in most cases be shown to violate the pumping conditions.

2. Models and methods

Quantum chemical calculations were performed on a model of the BNC in the A-family CcO to describe the main steps in the catalytic cycle, compare the scheme in Fig. 2. In the first subsection below the model of the BNC used in the calculations is shortly described, and in the second subsection the quantum chemical methods used are described. In the final subsection the procedure used to connect the calculated relative energies to the experimentally known overall energies is described.

2.1. Model of the BNC and structure of the intermediates

The binuclear active site (BNC) in cytochrome c oxidase consists of a heme group in close vicinity of a histidine ligated copper complex (Cu_B). The model used in the calculations is based on a recent crystal structure from *Rhodobacter sphaeroides* [9], see Fig. 3. The heme a_3 group is modeled by an unsubstituted porphyrin except that the farnesyl hydroxyl and the formyl groups are kept. The proximal histidine is also included in the model. The Cu_B model includes the three histidine ligands together with the cross-linked tyrosine. The amino acids are in most cases truncated at the alpha-carbon, which is fixed to the X-ray coordinates during geometry optimizations to maintain some of the constraints from the surrounding protein. The peptide bonds are replaced by C–H bonds, with the hydrogen atoms fixed. Two atoms on the porphyrin are also fixed. Three water molecules from the X-ray structure of CcO are included in the model together with simpler models of two threonines, hydrogen bonding to these water molecules. This procedure gives a model with about 144 atoms (depending on the state), see further ref. [38]. A larger model with about 200 atoms, including the propionate groups on heme a_3, two more amino acid residues, hydrogen bonding to the propionates (one arginine and one aspartic acid), plus three water molecules in this region, was also tried, and it was found to give similar results, not reported here.

Using the model shown in Fig. 3 the different intermediates in the catalytic cycle, as described in Fig. 2, are constructed by adding one electron and one proton for each reduction step, after the O–O bond cleavage. The purpose of the present paper is not to discuss possible different forms of the intermediates, but rather to discuss the energetics obtained from the structural forms of the intermediates as depicted in Fig. 2. However, a few comments should be made about these structures. As discussed in previous studies, it is found that leaving the tyrosine residue unprotonated until the final step, results in the most reasonable energy diagram [38,39], and this approach is therefore used here also. In the case of intermediate **O**, there is actually a very small energy difference between the tyrosinate and the tyrosine form. Another aspect of the intermediate **O** structure, is whether the hydroxyl group is on iron or on copper. In fact, the tyrosinate form of intermediate **O** can be described as two hydroxides, one on each metal, with a proton in between, strongly bound to both oxygens. This proton can move to either hydroxide group without large energy changes. In the present model the form having the hydroxyl group on copper and a water molecule on iron is

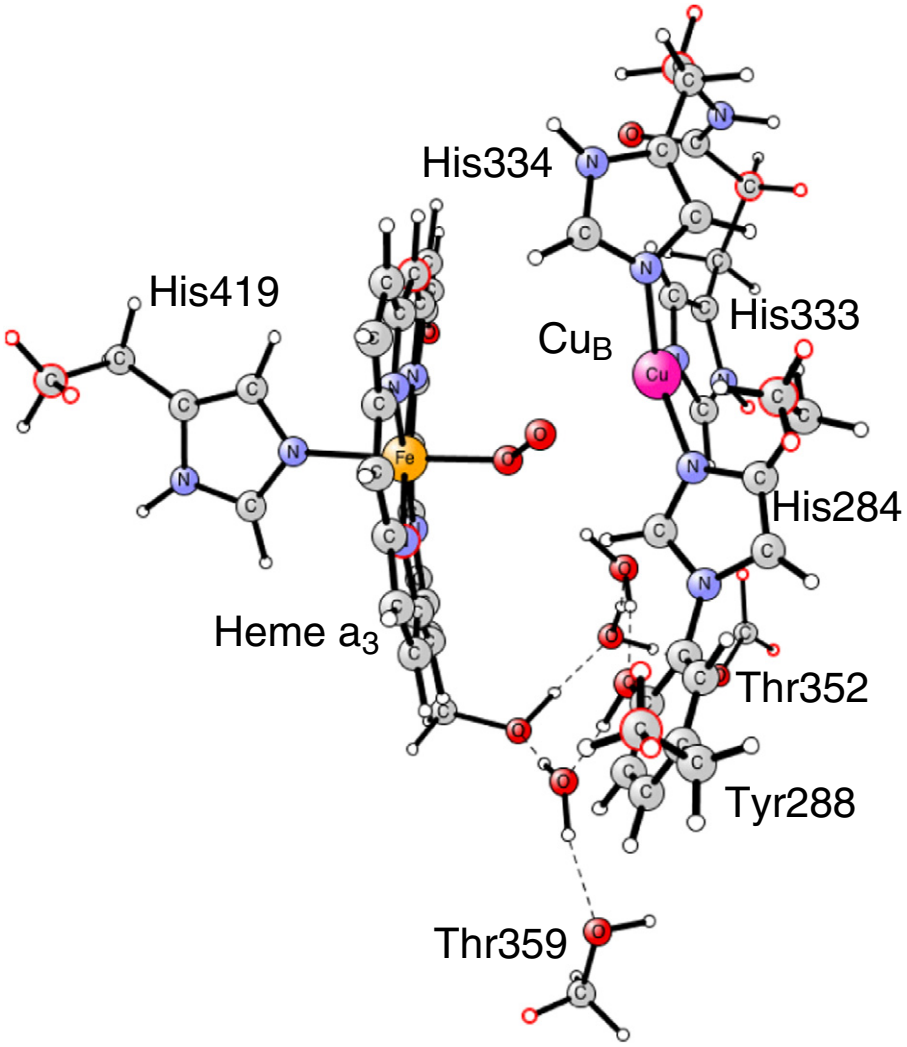

Fig. 3. Model of the BNC, built on the X-ray structure of the fully reduced CcO [9] (PDB:3FYE). The atoms with red circles are fixed to the X-ray coordinates in the geometry optimizations.

slightly lower in energy, and therefore the one shown in the diagrams. As mentioned elsewhere, based on experimental observations it has been suggested that there exist two different forms of intermediate **O**, labeled **O** and $\mathbf{O}_h$, where $\mathbf{O}_h$ should be an activated, energetically excited form [10,18,19]. The fact that the structure used in the present study is more or less the most stable one found, indicates that it should correspond to the unactivated **O** form. Therefore this notation, **O**, which could also be considered as a generic notation of this intermediate, is used in the manuscript. The fact that the **O** to **E** transition from the calculations seems to be more exergonic than expected [10], might indicate that the presently used structure could correspond to the activated $\mathbf{O}_h$ form. Another aspect of the intermediate structures concerns the water molecules in the BNC. The model used is built on an X-ray structure of the fully reduced enzyme with unusually many water molecules in the BNC [9]. Although the structure of each intermediate is fully optimized, it is difficult to know if the global minimum with regard to the water molecules has actually been obtained in each case. However, it is expected that the water molecules should have minor effects on the calculated relative energies.

2.2. Computational methods

Quantum mechanical calculations were performed on the BNC model employing the hybrid density functional B3LYP [40] and the re-parameterized B3LYP* functional, which uses 15% Hartree–Fock exchange as compared to the 20% used in the original functional [41]. All structures were fully optimized, except for some atoms fixed from the crystal structure as discussed above, using the B3LYP functional and the double zeta basis set labeled lacvp in the Jaguar program [42]. Single point calculations were performed in the optimized structures using the large cc-pvtz(−f) basis set plus lacv3p+ for the metal ions with both the B3LYP and the B3LYP* functional. Single point dispersion effects were included, using the empirical formula by Grimme [43], since it has been shown that the lack of dispersion in DFT theory may lead to large errors when molecules are forced closer to each other [43,44]. Solvent effects from the surrounding protein were included using the self consistent reaction field (SCRF) approach as implemented in Jaguar with a dielectric constant of 4.0, in accordance with previous experience [45]. The dielectric calculations were performed for the optimized structures using the B3LYP functional and the lacvp* basis set, which has polarization functions on all second row atoms. The program Jaguar 7.6 [42] was used in all calculations described so far.

Several benchmark tests on the accuracy of the B3LYP functional have been performed [46], and based on those results an error of 3–5 kcal/mol is expected for the computed relative energies for transition metal containing systems [47].

In all optimized structures the Hessian matrix, i.e. second derivatives of the energy with respect to the nuclear coordinates was calculated using the Gaussian 09 package [48] at the same level of calculation as the geometry optimizations (B3LYP/lacvp). The Hessians were used to calculate zero-point corrections, but due to the fixed coordinates in the geometry optimizations, entropy effects would not be reliable and could not be taken from the Hessian calculations. The entropy changes within the BNC itself can rather safely be assumed to be small and therefore negligible. The main entropy changes occur when molecules enter or leave the system, and these have to be estimated in some approximate way. For the gaseous O_2 molecule it is assumed that the entropy lost on binding is equal to the translational entropy for the free molecule (10.8 kcal/mol at room temperature). For the binding of a water molecule to bulk water a standard value of 14 kcal/mol is used.

The relative energies reported below are referred to as free energy values, with entropy effects estimated as described in the previous paragraph. The enthalpy values are obtained from the large basis set calculations using the B3LYP* functional, including zero point effects, dispersion and solvent effects. Using the B3LYP results instead of B3LYP* gives a similar picture. Due to uncertainties in the calculated spin-state splittings for heme-iron, a correction of 4.6 kcal/mol is introduced increasing the Fe(II) ionization potential. The value is chosen to improve the agreement with experiments for the O_2 binding step in CcO. This correction makes the relative energies reported here somewhat different from those reported previously [38]. Furthermore, the previously reported values lack both dispersion and zero-point effects. The correction used here is also slightly different from the one used for CcO in a recent study mainly concerned with nitric oxide reductase [49].

2.3. Overall energetics, barriers and effects of the gradient

To obtain an energy diagram for a full catalytic cycle of CcO the energetics of the reduction steps has to be calculated. This means that the redox potentials of the active site have to be compared to the redox potential of the electron donor, and the pK_a values of the active site have to be compared to the pK_a value of the proton donor, i.e. bulk water. To use quantum chemical methods to calculate redox potentials and pK_a values implies the calculation of electron and proton affinities, properties which are strongly dependent on the surroundings since the charge is changed. Therefore the SCRF approach, which works very well for calculations of relative energies with constant charge, is not accurate enough to give absolute electron and proton affinities. However, relative redox potentials and pK_a values for the same site (such as the BNC) can be calculated with much higher accuracy, since the surroundings are the same in all steps. These difficulties in calculating accurate absolute redox potentials and pK_a values prompted us to develop a different procedure, which has been used in several similar cases [15–17,37,50,51]. By adjusting the calculated energetics of the entire catalytic cycle to the total reaction energy obtained from experimental reduction potentials, accurate energy diagrams can be obtained, where every second step in the reduction procedure, i.e. transferring both an electron and a proton, is determined. It can be noted that this procedure does not make up for possible imbalances in the DFT-description of reduction potentials involving different oxidation states and different metals.

Using experimental midpoint reduction potentials for the electron donor and acceptor, 0.25 V for cytochrome c and 0.8 for reduction of O_2 to water, and considering that four electrons are involved, the exergonicity of one catalytic cycle of CcO becomes 51.0 kcal/mol (2.2 V) [14]. In combination with the calculated free energy for the chemistry occurring in Eq. (1), the cost of each reduction step (transfer of one electron from the donor and one proton from the bulk) can be set to yield the total experimental exergonicity. This determines the energetics for each of the reduction steps in the catalytic cycle.

To make a kinetic analysis possible, also barriers for the different reaction steps must be included in the energy profile for the entire catalytic cycle. For the O–O bond cleavage barrier, an accurate value of 12.4 kcal/mol, is obtained from an experiment [52], deduced from the life-time of compound **A** using transition state theory. Each reduction step involves several elementary steps of electron and proton transfer, but when the entire catalytic cycle is considered each reduction step is described in a simplified way with a single rate limiting barrier for the charge (electron and proton) transfer processes. The reaction rates for the different reduction steps are in the 100 to 1000 μs range, and for the present type of qualitative discussion it is enough to use the same approximate value of 13.0 kcal/mol, without gradient, in all reduction steps for the rate limiting barrier of the elementary charge transfer steps.

The presence of the electrochemical gradient across the membrane will affect both the relative energies of the intermediates in the CcO reaction, and the barrier heights. The intermediates are affected since the movement of charge against the gradient is endergonic, in contrast to the situation without gradient, where there is no cost connected specifically with the movement of the charges. The maximum gradient is known from experiments to be 200 mV (4.6 kcal/mol) [14], which means that the full gradient adds an extra cost of 4.6 kcal/mol for each charge moved against the gradient across the membrane. Thus the effects of the gradient on the relative energies of the intermediates can

easily be estimated, since only charge transfer steps across the entire membrane need to be considered. The effect of the gradient on the rate limiting charge transfer barrier should depend on the particular mechanisms involved in the charge movement. Here it is considered reasonable to increase the barrier by 1.5 kcal/mol at 100 mV and by 3.0 kcal/mol at the full gradient of 200 mV.

3. Results and discussion

The results of the present investigation are reported in three different subsections below. In the first subsection, 3.1, the energetics of the entire catalytic cycle is discussed and the requirements for proton pumping in all four reduction steps are evaluated. In the second subsection, 3.2, details of the proton pumping mechanism are discussed and developed, based on energy profiles for individual reduction steps. In the final subsection, 3.3, the variation in proton pumping stoichiometry between different subfamilies of cytochrome oxidase is discussed.

3.1. Requirements for proton pumping in all four reduction steps in cytochrome c oxidase

In this section the energetic requirements for proton pumping in cytochrome c oxidase are discussed on the basis of the energetics of the entire catalytic cycle, described in Eq. (1) and in the more detailed scheme in Fig. 2. It is shown that, using the present knowledge of the thermodynamic and kinetic properties of the oxygen reduction reaction in CcO, pumping of one proton per electron can occur at low gradient and up to approximately half the maximum gradient. At higher gradients, a quite efficient energy conservation can still be obtained if the proton pumping is uncoupled *only* in the least exergonic reduction steps. So far, mainly the thermodynamic aspects of the catalytic cycle have been discussed in the literature, but to understand the requirements for proton pumping also kinetic aspects have to be considered. In this section, where the energetics of the entire catalytic cycle is considered, each reduction step will be described in a simplified way, with all elementary electron and proton transfer steps merged together and shown as a single rate-limiting barrier. To fully understand the specific mechanisms for the proton pumping, each reduction step has to be described in much more detail, including barriers for all individual electron and proton transfer steps, which will be done in the next section below (3.2).

As mentioned above, the overall thermodynamics for the CcO reaction can be obtained from the reduction potentials of the donor, cytochrome c, and the acceptor, molecular oxygen, yielding an exergonicity of 51.0 kcal/mol for one catalytic cycle [14]. The main part of the exergonicity is expected to arise in the reduction steps, which are all equivalent in the sense that each step involves the uptake of one electron and one proton, together with the pumping of one proton across the membrane, see the scheme in Fig. 2. However, energetically the four reduction steps are not equivalent since according to experimental information the redox potentials of the specific electron (and proton) acceptors are not the same [10,13,19]. On the contrary, two of the reduction steps in the scheme in Fig. 2 seem to have a very low exergonicity, and as mentioned in the introduction this result has been interpreted to be incompatible with other experimental observations that proton pumping actually occurs in all four reduction steps [18,21,22].

In the present study the energetic requirements for proton pumping in all four reduction steps are scrutinized by constructing a tentative free energy profile of the entire catalytic cycle, involving not only the thermodynamics, but also the rate limiting barriers for the charge transfer reactions in each reduction step as well as for the O – O bond cleavage step, see Fig. 4. As discussed in the introduction, by a combination of electrogenic chemistry and proton pumping a significant part of the free energy of the exergonic reaction is conserved as an electrochemical gradient across the membrane, which means that when the gradient has started to build up, all charge transfer steps become less exergonic. This variation in the energetics has to be taken into account in the energy analysis. The effect of the gradient on the energetics can rather easily be estimated, see Section 2. As will be discussed in detail below, the orange energy profiles in Fig. 4 show that one effect of the gradient is to increase the barriers, leading to a decrease in the rate of the reaction.

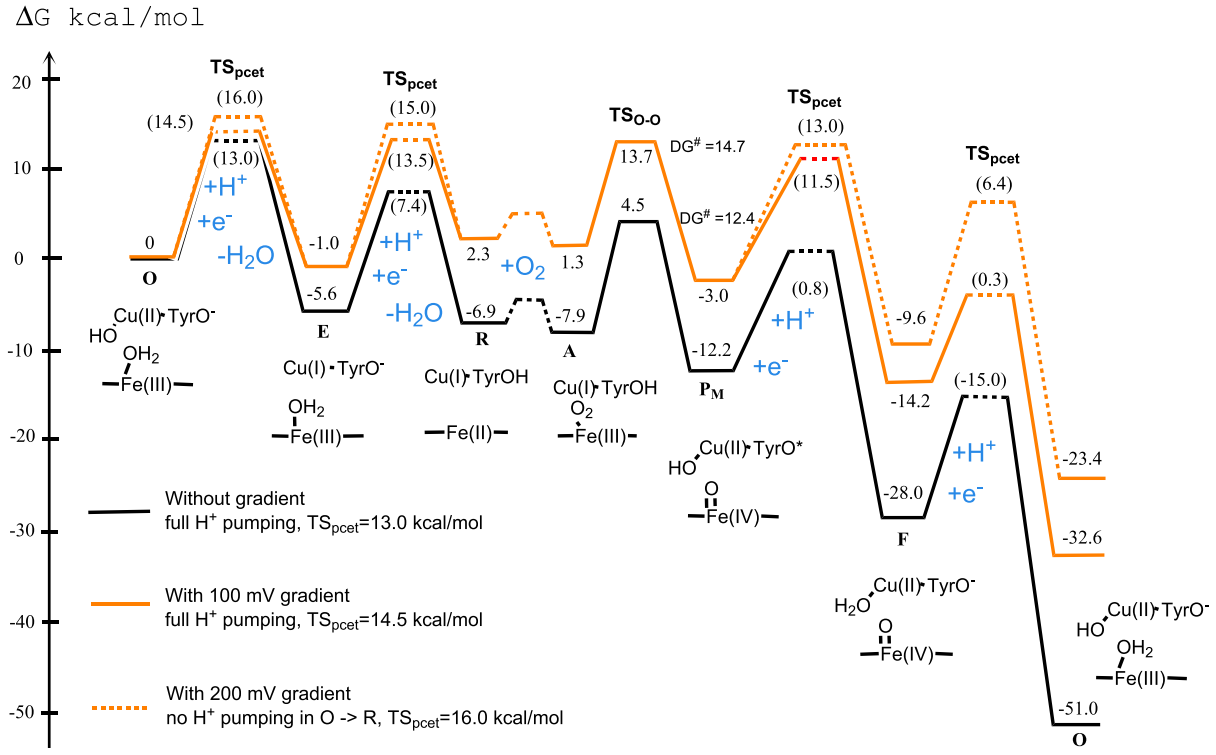

Fig. 4. Calculated free energy profile for the catalytic cycle of CcO, black curve. The orange curves correspond to the situation with the gradient present, see further in the text.

Reactions with too high barriers must be excluded. It should be stressed here that the barrier connected with a particular transition state (**TS**) always has to be calculated relative to the lowest preceding point on the energy profile.

Using the models and quantum chemical methods described in Section 2, the relative energies of all the intermediates in the reaction scheme in Fig. 2 were calculated. The results are shown as the black energy profile in Fig. 4, which has the oxidized state labeled **O** as reference point. As mentioned in Section 2 above, the generic notation **O** is used here, since it is not possible to determine which of the different forms of the fully oxidized intermediates the calculations correspond to. The calculated relative energies agree quite well both with the general picture obtained from experimental results discussed above [10,13,19], and with previously published calculated results [15–17]. Starting from the oxidized state **O** the BNC is reduced to state **R** with Cu(I) and Fe(II), in two steps which are only weakly exergonic, in the range 1.3 to 5.6 kcal/mol. Molecular oxygen binds to state **R**, and together the binding and the cleavage of the O–O bond are weakly exergonic. A free energy value of −5.3 kcal/mol is obtained for $\mathbf{P}_M$ relative to the reduced state, **R**. These steps, the binding and cleavage of O_2, do not involve any charge transfer perpendicular to the membrane. The first two reduction steps after the O–O bond cleavage, the annihilation of the tyrosyl radical ($\mathbf{P}_M$ to **F**) and the reduction of Fe(IV) to Fe(III) (**F** to **O**) are quite exergonic, with values in the range 15.8 to 23.0 kcal/mol, see Fig. 4. In the figure, the proton (and electron) transfer barriers are also included, as well as the O–O bond cleavage barrier. As described in Section 2 these barriers are not calculated but estimated on the basis of experimental data. Furthermore, a small entropy barrier for the O_2 binding step is included, to make the energy profile complete. The black curve in Fig. 4 thus corresponds to the situation without any gradient across the membrane, which means that there is no cost for proton pumping, and also no extra cost for the electrogenic uptake of protons and electrons. Clearly, the most interesting situation is with a gradient present, and therefore two more energy profiles are shown in Fig. 4, where the energetic effects of the gradient (two different values) have been added according to the procedure described in Section 2.

Several conclusions can be drawn from the energy profiles in Fig. 4. First, consider the energy profile without gradient (the black curve), which should correspond to the situation in many experiments, e.g. investigating the presence of proton pumping in individual steps of the catalytic cycle. Since there is no cost of proton pumping without gradient, and since all steps are exergonic, from a thermodynamic point of view there is nothing that prevents proton pumping to occur in all steps, because even a very small exergonicity is enough to drive each reaction step forward. Furthermore, also from a kinetic point of view, there is nothing in this energy profile that prevents proton pumping to occur in every reduction step, since the fact that all steps are exergonic makes the rate limiting barrier in each step determined by the local barrier. It can also be noted that the same conclusions should be drawn, even if the **O** to **E** transition would have a lower exergonicity, of the same order as the **E** to **R** transition, i.e. if the calculated state **O** would correspond to the activated state $\mathbf{O}_h$. Therefore, with this energy profile, and at this level of details in the thermodynamic and kinetic analysis, the lack of proton pumping observed under some experimental circumstances in the reduction steps with low exergonicity [18], is difficult to understand. Clearly, the present investigation cannot exclude that there exists some kind of activated forms of states **O** and **E**, which has been proposed, to explain the observed differences in proton pumping efficiency under different experimental conditions [18,21], but it indicates that, from a purely thermodynamic point of view, such activated forms should not be needed for proton pumping to occur in all steps when there is no gradient present.

The second energy profile in Fig. 4, the full orange curve, is obtained from the black curve by adding the energetic effects from a gradient of 100 mV across the membrane, and assuming that one proton is pumped in each of the four reduction steps. This value of the gradient, half the maximum gradient, is chosen to give a qualitative picture of the effects of the gradient, since as discussed below, the calculated energy profile is not accurate enough to make a detailed comparison to any particular experimental results. It is interesting to note that even with this gradient present, all reduction steps but one, **E** to **R**, are exergonic. Most importantly, this means that the rate of all reduction steps is affected only by the direct effect from the gradient on the local proton (and electron) transfer barriers, and not by any previous endergonic step. The only barrier affected by a previous endergonic step is the O–O bond cleavage barrier, which in itself is not affected by the gradient, since there is no motion of charges perpendicular to the membrane for this step. As can be seen from Fig. 4 the total O–O bond cleavage barrier is only 14.7 kcal/mol, which is very similar to the proton transfer barriers assumed to be 14.5 kcal/mol at this gradient. Furthermore, the fact that the O–O bond cleavage step (**R** to $\mathbf{P}_M$) is exergonic by 5.3 kcal/mol, and not affected by the gradient, ensures that the following steps are not affected by any previous weakly endergonic steps. It can be concluded that with the energy profile presented in Fig. 4, it is still possible to pump one proton in all four reduction steps when the gradient has increased to 100 mV, without decreasing the rate more than that due to the intrinsic effects on the proton transfer barriers, i.e. there is no "extra" endergonicity increasing the barriers due to the low original exergonicity in two of the reduction steps.

The third energy profile in Fig. 4, the dashed orange curve, is obtained from the black curve by adding the energetic effects from a gradient of 200 mV across the membrane, i.e. the maximum gradient, and by assuming that only the two most exergonic reduction steps pump protons. As can be seen from Fig. 4, with half the maximum gradient the two reduction steps from **O** to **R** together results in a slightly endergonic reaction (+2.3 kcal/mol). This means that with a further increase of the gradient these two steps will become more endergonic, and with the full gradient and continued full proton pumping for these steps the endergonicity would be 11.5 kcal/mol. This endergonicity in itself would be no problem, since the following steps would continue to be exergonic and drive the process forward. However, since the endergonicity would also significantly increase the rate limiting barriers, both for the proton transfer step from **E** to **R**, and for the O–O bond cleavage step (22.9 kcal/mol), the process would become too slow. Clearly, if the reduction steps **O** to **R** could be made more exergonic by using some energy from the previous more exergonic reduction steps, this problem could be solved. At least about 7 kcal/mol needs to be transferred in this way, which would result in a more reasonable increase of the total O–O bond cleavage activation energy to 16 kcal/mol. However, it should be noted that with the present energy values, at least half of the energy saved would have to be saved in the **E** intermediate, since an exergonic **O** to **E** step would be a waste, since it would add to the total barrier. As discussed above, there is no experimental support for how such energy transfer between the reduction steps could occur, and therefore an alternative solution is suggested here. A similar decrease of the endergonicity of the two reduction steps from **O** to **R** at high gradient could be obtained if the proton pumping is uncoupled in these two steps when the gradient reaches a certain value. A value for the gradient somewhat larger than 100 mV would still allow for a reasonably fast process, pumping one proton in all reduction steps, but the uncertainties in the calculated energy profile do not allow an accurate determination of the limits for the proton pumping with respect to the value of the gradient. Therefore, apart from the energy profile for half the maximum gradient, in which case it seems to be quite certain to conclude that four protons per oxygen molecule can be pumped without significantly decreasing the rate of the reaction, as discussed above, a second limiting case is also shown in Fig. 4. In this case it is assumed that at full gradient only two protons per oxygen molecule are pumped, to prevent that the reaction becomes too slow, as discussed in the following paragraph.

The dashed orange curve in Fig. 4, constructed as described above, has exactly the same characteristics as the full orange curve at a gradient

of 100 mV discussed in the paragraph above. This means that the rate for the proton transfer steps are only determined locally, and the only barrier affected by a previous endergonic step is the O – O bond cleavage barrier, which again becomes 14.7 kcal/mol, and it is thus lower than the proton transfer barriers which are assumed to be 16.0 kcal/mol at this gradient. An important aspect is that the proton pumping can be specifically uncoupled *only* in the two least exergonic steps at higher values of the gradient. To increase the proton leakage equally in all reduction steps would not be as efficient. It is shown in the next Section (3.2) how this type of redox dependent uncoupling of proton pumping could occur. It should also be noted that when the gradient increases, the barriers for the allowed reaction steps that involve both chemistry and proton pumping increase, making the differences between these barriers and the barriers that control the gating smaller, and thereby the gating becomes less efficient.

The analysis above is made using the simple assumption that the computed relative energies for the reduction steps are realistic and that each reduction step can be described by a simplified rate limiting barrier of 13 kcal/mol (with no gradient). It should be noted though, that there might be a limit for how small the exergonicity can be to allow a reasonable pumping mechanism. In fact, for the pumping mechanism described in the next Section (3.2), an exergonicity of about 5 kcal/mol is needed for the entire reduction step. Otherwise the rate of the reduction step would be slowed down further because of internal endergonic steps within the reduction step, see further next section. This might indicate that the calculated energy profile, with an exergonicity of only 1.3 kcal/mol for the **E** to **R** step, has a somewhat too small exergonicity for this step to allow proton pumping at the expected rate. The missing energy, 3–4 kcal/mol, is certainly within the error bars of the calculated reduction potentials/pK_a-values. The uncertainties connected with the description of the release of the newly formed water molecules are also worth mentioning.

In summary, based on quantum chemical calculations, using the most accurate methodology available for this kind of system, and some experimental information concerning rates of observed reaction steps, a free energy profile, including proton transfer barriers, for the entire catalytic cycle of CcO has been constructed. The calculated relative energies of the reaction intermediates agree with experimental indications that two of the reduction steps, **O** to **E** and **E** to **R**, are significantly less exergonic than the first two reduction steps after the O – O bond cleavage. It is shown that the energy profile can be compatible with proton pumping in all four reduction steps with a gradient across the membrane present, at least up to half the maximum gradient. It is also shown that for a gradient close to the maximum value, the energy profile is still compatible with the pumping of two protons per oxygen molecule, with the uncoupling of proton pumping occurring specifically *only* in the two least exergonic steps, but it is not compatible with proton pumping in all four reduction steps at full gradient.

3.2. The proton pumping mechanism of cytochrome c oxidase: the presence of two proton channels enables redox dependent leakage

An important requirement for a pump mechanism is that the description of the elementary reaction steps of proton transfer is connected to an energy diagram showing how the barrier heights at different stages of the reaction govern the protons to move in the right direction [7,29,30]. In this section the previously constructed pumping diagram is developed further to include the observed differences between the different reduction steps. An essential ingredient in the basic pumping mechanism discussed here, is the assumption that the uptake of the pump-proton to the PLS drives the actual reduction and protonation of the BNC. The simplest way to obtain an uncoupling of the proton pumping under certain circumstances is then to allow the PLS proton to leak, either back to the N-side of the membrane or into the BNC, rather than being pumped to the P-side. With two proton channels one can have different mechanisms for proton transfer to the BNC. It is shown here that the different amino acid compositions of the D- and the K-channels makes it natural to assume that the barrier heights for proton transfer to the BNC in the two channels have a different dependence both on the redox properties of the BNC, and on the presence of an electrochemical gradient across the membrane. From the new diagrams constructed here it is possible to understand why the two proton channels are needed. It is also possible to suggest a mechanism for a redox dependent proton leakage.

The first realistic energy profile for one reduction step including not only the actually occurring steps, but also the non-allowed steps not leading to proton pumping, was constructed in 2007 [29]. It was based on the results from a kinetic experiment on a single reduction step in CcO (**O** to **E**) [28]. Similar diagrams have also been published in [11,17,53,54]. These pumping diagrams correspond to the situation with no gradient present, and they are constructed using a combination of experimental results and general principles for how a gating of protons can be achieved. To construct the diagrams, an important piece of experimental information used is that the allowed reactions occur on a ms time-scale. This means that, without gradient, the barriers for the proton transfer steps should not be higher than approximately 13 kcal/mol. Furthermore, to obtain a gating situation for the proton motion, the leakage pathways should be on the order of 100 times slower (without gradient), which means that the non-allowed reaction paths, not leading to proton pumping, should have barriers at least 2–3 kcal/mol higher than the allowed reaction path for chemistry and proton pumping. One important conclusion that could be drawn from the pumping diagrams was that the transition state for the initial uptake of the pump-protons to the PLS should be positively charged, to prevent back leakage of the protons to the N-side when the chemistry is completed [11,30,38]. Such a positively charged transition state could be obtained by an immediate reprotonation of the glutamic acid (Glu286) assumed to be essential for proton transfer in the D-channel [11,30,38]. However, even if the energy profile constructed was based on experiments on a particular reduction step, it was used as a generic diagram considered valid for any reduction step, since it was fitted to an average overall exergonicity. An important limitation to the previous diagram is that there is no part in the diagram that depends on the specific redox properties of the BNC. Furthermore, it does not take into account the experimental observation that two different proton channels are involved in the proton uptake to the BNC.

In the present study, the previously suggested energy diagram for one reduction step [11,17,29] is developed further to include the variation in redox properties of the BNC for different reduction steps as best known at present from experiments and computations. The general results from the kinetic experiment [28] and the most important interpretations of those results are still used. The general type of pumping mechanism is kept from the previous suggestions [11,17,29]. Thus, like the previously published pumping diagram, also the new diagrams constructed here are mainly based on experimental knowledge (the allowed reaction paths) with only a few theoretically motivated assumptions. An interesting observation is that the reduction steps with a low driving force are the ones that use the K-channel for the proton uptake to the BNC, while those with a large driving force use the D-channel. It is suggested here that two types of pumping diagrams are needed, differing in the overall exergonicity, and also in the parts that involve the actual electron and proton transfer to the BNC. Two different cases are therefore considered. The first one has a large driving force for the entire reduction step, set to 15 kcal/mol, see Fig. 5, which should qualitatively correspond to the two first reduction steps after the O – O bond cleavage, in which the D-channel is used for proton uptake to the BNC. The second diagram has a smaller driving force, set to 6 kcal/mol, see Fig. 6, which should correspond to the reduction step **O** to **E** for which the kinetic experiment was done [28], and for which the K-channel is used for proton uptake to the BNC. Using these two pumping diagrams, it is possible to suggest a mechanism that explains why the D-channel cannot be used for proton uptake to the BNC in all reduction steps. It is also shown that the use of

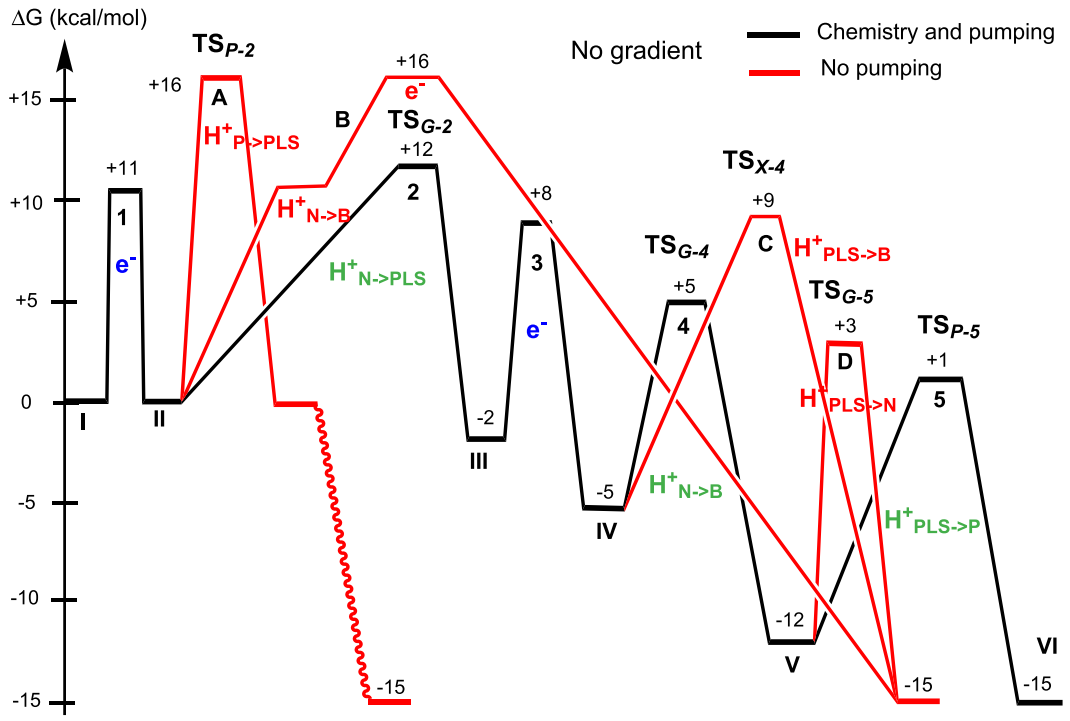

Fig. 5. Energy diagram (without gradient), assuming a 15 kcal/mol driving force, corresponding to the P to O reduction steps in CcO, showing both allowed (black) and non-allowed (red) pathways. The step numbers 1–5 are described in Fig. 1. The states labeled I to VI are described in the text. The transition states TS_G, TS_P and TS_X are indicated in Fig. 1.

two proton channels with different mechanisms for proton transfer to the BNC enables a redox dependent proton leakage from the pump loading site, PLS, to the BNC at a high gradient. This result was used in the previous section, where it was shown that an efficient energy conservation can be obtained, if proton leakage occurs *only* in the reduction steps with weak exergonicity.

To introduce the new features in the proton pumping mechanism, the main properties of the previously published mechanism and the procedure for construction of the energy profile need to be summarized. The first step in the reaction, electron transfer from Cu_A to heme a, step 1 in Fig. 1, from I to II in Figs. 5 and 6, is the same in all cases and the barrier, 11 kcal/mol, is taken from the kinetic experiment [28]. The electron

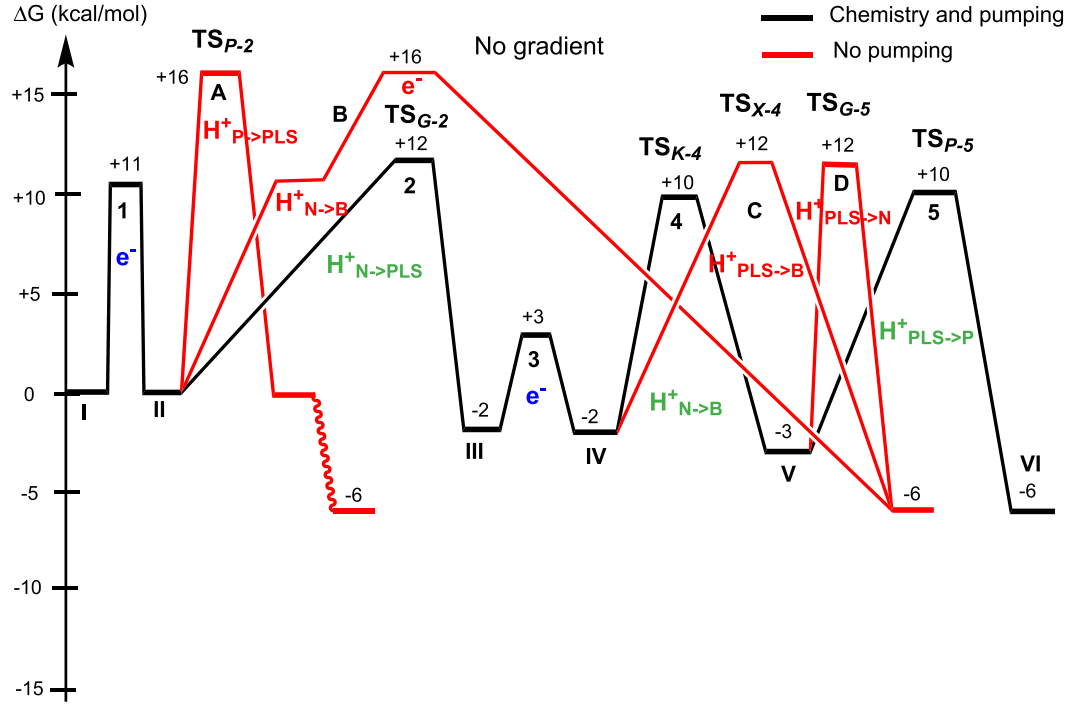

Fig. 6. Energy diagram (without gradient), assuming a 6 kcal/mol driving force, corresponding to the O to E reduction step in CcO, showing both allowed (black) and non-allowed (red) pathways. The step numbers 1–5 are described in Fig. 1. The states labeled I to VI are described in the text. The transition states TS_G, TS_P, TS_K and TS_X are indicated in Fig. 1.

on heme a triggers the uptake of a proton from the N-side, via the transition state TS_{G-2} (TS_G in Fig. 1) to the pump loading site (PLS), and also this step, step 2 in Fig. 1, from II to III, is the same in all reduction steps. An important result from the kinetic experiment was that the barrier for this proton uptake is quite high, here set to 12 kcal/mol, which corresponds rather closely to the observed rate. The most important gating situation at this point is labeled A in the diagrams (Fig. 5 and 6) and concerns the competing uptake of the proton from the P-side, which is prevented by the high barrier at 16 kcal/mol via the transition state TS_{P-2} (TS_P in Fig. 1). The height of this barrier, 16 kcal/mol in both diagrams, is obtained from the reverse of step 5 in Fig. 1, from VI to V in Figs. 5 and 6. The proton uptake to the PLS is set to be exergonic, since this state was observed in the experiment on the **O** to **E** reduction step, and the value is chosen to be −2 kcal/mol. This value is also determined by a later gating situation.

The next step, electron transfer from heme a to the BNC, step 3 in Fig. 1, from III to IV, is followed by the proton transfer from the N-side to the BNC, step 4 in Fig. 1, from IV to V. Clearly, the energetics of these two steps, electron and proton transfer to the BNC must depend on the redox properties of the specific acceptors in the BNC, and this is where the two diagrams in Fig. 5 and Fig. 6 become different from each other. In the **O** to **E** and **E** to **R** transitions the electron transfer to the BNC is assumed to be fast, with a barrier of 5 kcal/mol taken from the kinetic experiment [28]. In these two cases the electron goes from Fe(II) on heme a to either Fe(III) or Cu(II) in the BNC without much rearrangements needed. In the $\mathbf{P}_M$ to **F** and **F** to **O** transitions, where the electron goes to the tyrosyl radical or to the ferryl group, the electron transfer barrier is expected to be higher, either because the involvement of a high energy state, or because of structural rearrangements in the BNC involving proton transfer. In the reduction steps with a high reduction potential, shown in Fig. 5, the electron and proton transfer steps together should be exergonic by 10 kcal/mol to give an overall exergonicity of 15 kcal/mol of the entire reduction step. To achieve this, the electron transfer is set to be exergonic by 3 kcal/mol, and the proton transfer to BNC by 7 kcal/mol. In the less exergonic reduction steps, Fig. 6, the electron transfer is set to be thermoneutral, which is in agreement with the kinetic experiment performed for the **O** to **E** transition. The proton transfer should be only weakly exergonic, and is set to 1 kcal/mol. This large difference in exergonicity of steps 3 and 4, corresponding to the actual reduction of the BNC, is also likely to lead to different barrier heights for proton transfer to BNC, such that the more exergonic step will have a lower barrier, here set to 10 kcal/mol, than the less exergonic step, here with a barrier set to 12 kcal/mol. The latter value is close to the result obtained in the kinetic experiment [28]. The gating situation for these steps, labeled C, presents a new possibility to differentiate between the reduction steps. This step and its barriers will be discussed below.

Before discussing the uptake of the BNC proton, the energy profile for the full reduction step will be completed. The last reaction step in the diagram describes the expulsion of the proton from the PLS, via transition state TS_{P-5}, to the P-side, step 5 in Fig. 1, from V to VI, due to the repulsion from the BNC proton. This step should be the same in all reduction steps, with a barrier that should thus be 13 kcal/mol. With the exergonicity set to 3 kcal/mol for this step, the reverse barrier for leakage from the P-side becomes the required 16 kcal/mol, which is used in gating situation A discussed above. In this last step, V to VI, the gating situation labeled D corresponds to preventing the proton in the PLS to leak back to the N-side, via transition state TS_{G-5}, instead of being pumped to the P-side via transition state TS_{P-5}. This is where the positive character of transition state TS_G plays its role. Transition state TS_{G-2} (Fig. 5 and 6) for the uptake of the proton to the PLS from the N-side has to be low enough to allow this reaction rather than the one taking the proton from the P-side. With a positive charge, the transition state is stabilized by the electron on heme a, compare Fig. 1, during the step 2, from II to III [11,30]. On the other hand, in gating situation D, there is no uncompensated negative charge in or near the BNC. Therefore, the positively charged transition state TS_{G-5} remains high, and prevents back leakage of the proton to the N-side. The pK_a in both PLS and TS_{G-5} is raised when the negative charge in heme a is quenched. It is here assumed that the distance between transition state TS_G and heme a is slightly smaller than the distance between the PLS and heme a, which means that the transition state is slightly more affected by the negative charge than the PLS. The back leakage barrier TS_{G-5} should therefore be 15 kcal/mol, slightly higher than the reverse barrier from III to II via TS_{G-2}. This barrier of 15 kcal/mol should be more or less enough to prevent leakage. Proton pumping to the P-side via the 13 kcal/mol high TS_{P-5} barrier should therefore be the promoted reaction.

The discussion above is essentially a summary of previous suggestions for the pumping mechanism in CcO, apart from the details of the proton uptake from the N-side to the BNC, which will be developed further here. For the first two reduction steps after the O – O bond cleavage, it is known from experiments that the chemical proton (going to the BNC) is taken up via the D-channel [32,33]. The transition state TS_{G-4} has commonly been suggested to involve a glutamic acid, Glu286, known to be protonated at physiological pH. The protonation of the BNC is suggested to be initiated by a deprotonation of Glu286, with the proton moving towards the negative charge in the BNC [30,55]. Clearly, when the proton transfer to the BNC is involved in a strongly exergonic reaction step, as the one shown in Fig. 5, the TS_{G-4} barrier will be low and this reaction step will be fast. When the proton transfer to the BNC is involved in a more or less thermoneutral reaction step, on the other hand, this barrier will be higher. It is here suggested that it will be too high for the protons to be transferred through the D-channel, which is in accord with the experimental observations that in the **O** to **R** reduction steps, the BNC proton is rather taken up via the K-channel. It is here suggested that for the reduction steps with the low exergonicity, the barrier for proton transfer in the K-channel (with a transition state labeled TS_K, see Fig. 1), is lower than the barrier in the D-channel. The difference in character between the two transition states arises from the lack of an acidic residue inside the K-channel. Thus, due to the difference in character between the transition state TS_{G-4} in the D-channel and the transition state TS_{K-4} in the K-channel, the barrier for proton transfer in the K-channel is less dependent on the redox properties of the BNC than the barrier in the D-channel. Therefore, in the reduction step with high exergonicity, the TS_{G-4} is lower than the TS_{K-4}, and the D-channel is used, Fig. 5, while in the reduction steps with low exergonicity, the TS_{K-4} is lower than the TS_{G-4}, and the K-channel is used, Fig. 6, in accordance with experimental observations [32–34]. It should be noted that TS_{G-2} for proton transfer to the PLS is expected to have a different character than TS_{G-4} for proton transfer to the BNC, see further refs. [11,30,38].

The gating situation labeled C in Fig. 5 and 6 corresponds to preventing the pump-proton in the PLS to go to the BNC when the electron has arrived there, making sure that the proton is taken from the N-side. The fact that the desired proton uptake from the N-side occurs in different channels in different reduction steps also opens up the possibility for the gating situation to be different. One obvious pathway for leakage of the pump-proton to the BNC would be to go via transition state TS_{G-4}, i.e. the same transition state as for the proton coming to the PLS from the N-side. Since the proton in the PLS has a higher pK_a value than the protons on the N-side, the barrier from the PLS will be higher than the barrier from the N-side, which will prevent leakage and ensure that the BNC proton is not taken from the PLS but from the N-side and proton pumping occurs. This gating barrier is not shown in the energy diagrams in Figs. 5 and 6. However, the discussion in the previous Section (3.1) shows that it would be interesting to investigate if an efficient energy conservation can be obtained, if the PLS protons are allowed to leak into the BNC at high gradient, but *only* for the reduction steps with low exergonicity. Therefore, it is here suggested that there might exist another proton leakage path from the PLS to the BNC with a transition state labeled TS_X, see Fig. 1, and which has a barrier tuned to prevent all proton leakage at low gradient and to allow leakage in

some cases at high gradient. In the diagrams in Figs. 5 and 6 this barrier is set to 14 kcal/mol which should prevent leakage in all reduction steps without gradient across the membrane. It is suggested that the transition state TS_{X-4} is less affected by the increasing gradient than the transition state TS_{K-4}, which could be due both to their different positions in the membrane and to a difference in character. In this way, at a high gradient TS_{X-4} could be lower than TS_{K-4}, and the protons could start to leak from the PLS to the BNC in the reduction steps with low exergonicity. At the same time, the transition state for proton uptake in the D-channel, TS_{G-4}, used for the two reduction steps with high exergonicity, is significantly lower than the TS_{X-4}. Therefore, this transition state will stay lower than TS_{X-4} also for a high gradient, and there will be no proton leakage from the PLS to the BNC for these reduction steps.

As mentioned above, the pump diagrams discussed here correspond to the situation with no gradient present, and they are constructed using a combination of experimental results and general principles for how a gating of protons can be achieved. To prevent leakage of the protons requires high gating barriers, which in turn requires fairly high barriers for the allowed reactions, which is also in agreement with experimental rate determinations. Another consequence is that certain elementary steps must be exergonic by a few kcal/mol to obtain a large enough difference between the barriers for allowed and non-allowed reactions, which in two cases here are determined by the reverse barrier of an allowed forward reaction step ($TS_{G-2} \rightarrow TS_{G-5}$ and $TS_{P-5} \rightarrow TS_{P-2}$). With the present assumptions for acceptable leakage rates (less than 1%) an exergonicity of at least 5 kcal/mol for the entire reduction step is required. With a smaller exergonicity and the same assumptions for the local barrier heights, endergonic elementary reaction steps would occur, which would increase the barrier for the forward reaction, and thereby further decrease the rate of the reduction step. Furthermore, the inclusion of a gradient in the energy diagrams probably leads to additional constraints.

In summary, it is suggested that not only the thermodynamics, but also the barrier for proton uptake to the BNC depends on the redox properties for the specific acceptors in the BNC, and the barriers will therefore be different in both height and character in the different reduction steps. This can explain why the proton uptake to the BNC has to occur via the two channels, the D- and the K-channel, which have different chemical properties due to different amino acid composition. Furthermore, by introducing a new proton leakage path between the PLS and the BNC, it is also possible to explain how proton leakage at high gradient can be directed to occur only for the reduction steps with low exergonicity.

3.3. The varying stoichiometry of proton pumping in different families of cytochrome c oxidase

As discussed in the introduction, it has been found that it is mainly CcO from the A-family that pumps one proton per electron in the reduction process. The other families seem to have a lower stoichiometry in the proton pumping, even if the situation for one example of the C-family is somewhat unclear with different experimental results for different species [2,56–58]. At least for the B-family, it seems to be established that the stoichiometry is two protons pumped per catalytic cycle, i.e. 0.5 protons per electron [2]. As was also mentioned in the introduction, it has been suggested that this stoichiometry is reached by taking up the proton to the PLS in one reduction step and expelling it in the next reduction step [35]. With the assumptions made in the present study concerning the uneven distribution of the free energy released, this type of arrangement would be surprising, since it means that only one proton is pumped in the two very exergonic steps, and the other proton is pumped in the two steps which are only weakly exergonic. Furthermore, it is quite difficult to imagine how this kind of pumping scheme could work, and no mechanism has been suggested. Another difference between the oxidase families is that the A-family has two proton channels, labeled D and K, as discussed above, while the other families have only one, which usually is described as a K-channel analog. It has been suggested that the existence of only one proton channel is the reason for the lower pumping stoichiometry [2], but the question is how and why.

The redox dependent mechanism for leakage of protons from the PLS to the BNC at higher gradients, discussed in the previous section, actually presents an appealing possibility to explain how the reduced proton pumping in the B-family may be achieved. First, it should be realized that it might be better to describe the single proton channel in the B-family as a D-channel analog. This notation would be based on its functionality, rather than its location. Functionality here refers not only to the fact that the majority of the protons in the A-family are transferred via the D-channel, but also to mechanistic properties. The D-channel in the A-family has an important glutamic acid that is expected to play a role as initial proton donor, in particular for the proton transfer to the BNC. This residue is essential and conserved, except for a subclass of the A-family, where it is replaced by a tyrosine-serine motif (tyr-ser) that apparently can play the same role. The K-channel in the A-family has none of these residues (glu or tyr-ser), and therefore uses a different mechanism for the proton transfer. The single proton channel in the B-family, on the other hand, has the tyr-ser motif present, and it is therefore here suggested that the single proton channel in the B-family oxidases works in a way similar to the D-channel in the A-family. The results for the proton pumping mechanism in the A-family discussed above can therefore be applied to the B-family oxidases, considering that the only channel present corresponds to the D-channel.

Basically, one of the key results for the pumping mechanism discussed in the previous section for A-family oxidases, is that a possible role of the K-channel is to make proton pumping in the two least exergonic reduction steps possible, i.e. to increase the pumping stoichiometry from two to four protons pumped per oxygen molecule reduced. Thus, it is natural that without a correspondence to the K-channel in the B-family, there will be only two protons pumped per cycle. The key clue is the redox dependent barrier for proton transfer to the BNC suggested for the glu-dependent mechanism in the D-channel, which is here also suggested to be present for the corresponding tyr-ser mechanism in the B-family. For the first two reduction steps after the O – O bond cleavage, the proton transfer to the BNC is quite exergonic, and the barrier labeled TS_{G-4} in Fig. 5 is thereby quite low. The situation depicted in this figure should be valid for the first two reduction steps after the O – O bond cleavage in the B-family. However, for the other two reduction steps, proton transfer to the BNC is much less exergonic and the barrier is therefore higher. In the A-family there is the option to instead take up the protons via the K-channel, but for the B-family there is no such option. Instead, since the barrier for uptake of protons from the N-side is higher, the suggested leakage path via TS_{X-4} might be used, taking the protons from the PLS, and no protons would be pumped in these two steps. Thus, the two weakly exergonic reduction steps should be described by a modification of the diagram in Fig. 6, where the TS_{K-4} barrier is replaced by the TS_{G-4} barrier, which in this case is higher than the leakage barrier TS_{X-4}. In summary, the decreased proton pumping in the B-family would thus be caused by leakage of the protons from the PLS to the BNC in the least exergonic reduction steps.

It should be noted that the discussion in Section 3.1 above showed that it should be possible for the A-family CcO to pump four protons, even with the low exergonicity in two of the reduction steps. Clearly this means that the suggestion that the B-family pumps only one proton in the two strongly exergonic reduction steps and the second one in the two reduction steps with very low exergonicity cannot be dismissed for energetic reasons. But such an arrangement would probably require that pumping of the second proton stops at higher gradients, resulting in only one proton pumped per oxygen molecule. With the scenario suggested here, most likely, two protons can be pumped also at maximum gradient. It should also be noted that the changes of the metal cofactors between different CcO families might affect the details in the energy diagrams, which is not taken into account in the present discussion.

4. Conclusions

Different questions connected to proton pumping in cytochrome c oxidase are investigated in the present study using free energy profiles for the processes under examination. The reduction of molecular oxygen in cytochrome c oxidases, taking the electrons from cytochrome c, is exergonic by 51 kcal/mol, as obtained from experimental reduction potentials. Experimental reduction potentials also indicate that this free energy is quite unevenly distributed over the reduction steps, with a very low exergonicity in two of the four reduction steps. Still, it has been shown experimentally that in A-family cytochrome oxidases all four reduction steps are coupled to proton pumping. Therefore, it has been speculated that part of the free energy must be stored from the more exergonic reduction steps, to allow proton pumping in the less exergonic ones. To shed light on this apparent dilemma, free energy profiles for the entire catalytic cycle have been constructed, based on a combination of quantum chemical calculations (density functional theory) and experimental information. Since it is important to take into account both thermodynamic and kinetic aspects, estimated barriers for proton (and electron) transfer are included. By varying the amount of electrochemical gradient present, different profiles are obtained. From these energy profiles it can be concluded that, at least up to half the maximum gradient, it should be possible to pump one proton per electron, without substantial decrease in reaction rate, even with the low driving force in two of the reduction steps.

Several aspects of the proton pumping mechanism in cytochrome oxidase are still under debate. It is here argued that the only way to fully support a suggested mechanism is to provide energy profiles for the individual proton and electron transfer steps, showing that the allowed reaction steps involving both chemistry and proton pumping have lower barriers than reaction steps corresponding to proton leakage. In the present study a previously suggested mechanism for proton pumping in cytochrome oxidase is developed further to include redox dependent reaction energies and barriers. Therefore, two different energy profiles for an entire reduction step are constructed, one corresponding to the strongly exergonic reduction steps, experimentally known to use the D-channel for proton uptake to the BNC, and one corresponding to the weakly exergonic reduction steps, known to use the K-channel. These energy profiles are based on experimental information, electrostatic interactions and general principles for how proton pumping could occur. All important gating situations are considered. Important aspects of these energy profiles are that they suggest an explanation for the use of two proton channels in the A-family, and that they make it possible to suggest how a redox dependent proton leakage might occur at high gradient. The D- and the K-channels have different characters, in terms of types of amino acid compositions. This makes the properties of the rate limiting transition states for proton transfer to the BNC different for the two channels. The barrier in the D-channel is expected to become too high when there is a low driving force, and therefore the K-channel, with a transition state that depends less on the driving force, is used in those reduction steps. The already high barrier in the K-channel, on the other hand, will be more sensitive to an increase of the gradient than the low barriers in the D-channel, and therefore proton leakage at high gradient can occur exclusively in the reduction steps with low driving force.

Using the results for the A-family oxidases discussed above, it is also possible to suggest a new mechanism for the variation in proton pumping stoichiometry between the different subfamilies. It is suggested that the lower pumping stoichiometry observed for the B-family (and possibly also for the C-family) might be accomplished by uncoupling proton pumping in the weakly exergonic reduction steps, which in turn occurs by leakage of protons from the pump loading site to the BNC in these steps.

Finally it is noted that further studies are in progress, including attempts to evaluate the accuracy of the calculated relative reduction energies. Since the calculation of relative energies involving different oxidation states of the metals might not be accurately described by density functional theory, bench mark calculations are now in progress on smaller model complexes where also ab initio calculations can be performed. In this context, also a more detailed investigation of different possibilities for the form of each intermediate is undertaken.

References

[1] M. Wikström, Cytochrome c oxidase: 25 years of the elusive proton pump, Biochim. Biophys. Acta 1655 (2004) 241–247.
[2] H. Han, J. Hemp, L.A. Pace, H. Ouyang, K. Ganesan, J. Hyeob Roh, F. Daldal, S.R. Blanke, R.B. Gennis, Adaptation of aerobic respiration to low O_2 environments, Proc. Natl. Acad. Sci. U. S. A. 108 (2011) 14109–14114.
[3] B. Ludwig, Guest editor, special issue: respiratory oxidases, Biochim. Biophys. Acta 1817 (2012) 67–687.
[4] P. Brzezinski, G. Larsson, Redox-driven proton pumping by heme-copper oxidases, Biochim. Biophys. Acta 1605 (2003) 1–13.
[5] D.M. Popovic, A.A. Stuchebrukhov, Proton pumping mechanism and catalytic cycle of cytochrome c oxidase: Coulomb pump model with kinetic gating, FEBS Lett. 566 (2004) 126–130.
[6] K. Faxen, G. Gilderson, P. Ädelroth, P. Brzezinski, A mechanistic principle for proton pumping by cytochrome c oxidase, Nature 437 (2005) 286–289.
[7] M.H.M. Olsson, P.Z. Sharma, A. Warshel, Simulating redox coupled proton transfer in cytochrome c oxidase: looking for the proton bottleneck, FEBS Lett. 579 (2005) 2026–2034.
[8] A.V. Pisliakov, P.Z. Sharma, Z.T. Chu, M. Haranczyk, A. Warshel, Electrostatic basis for the unidirectionality of the primary proton transfer in cytochrome c oxidase, Proc. Natl. Acad. Sci. U. S. A. 105 (2008) 7726–7731.
[9] L. Qin, J. Liu, D.A. Mills, D.A. Proshlyakov, C. Hiser, S. Ferguson-Miller, Redox-dependent conformational changes in cytochrome c oxidase suggest a gating mechanism for proton uptake, Biochemistry 48 (2009) 5121–5130.
[10] V.R.I. Kaila, M.I. Verkhovsky, M. Wikström, Proton-coupled electron transfer in cytochrome oxidase, Chem. Rev. 110 (2010) 7062–7081.
[11] M.R.A. Blomberg, P.E.M. Siegbahn, The mechanism for proton pumping in cytochrome c oxidase from an electrostatic and quantum chemical perspective, Biochim. Biophys. Acta 1817 (2012) 495–505.
[12] M.M. Pereira, M. Santana, M. Teixeira, A novel scenario for the evolution of heme-copper oxygen reductases, Biochim. Biophys. Acta 1505 (2001) 185–208.
[13] G.T. Babcock, M. Wikström, Oxygen activation and the conservation of energy in cell respiration, Nature 356 (1992) 301–309.
[14] P. Brzezinski, Redox-driven membrane-bound proton pumps, Trends Biochem. Sci. 29 (2004) 380–387.
[15] P.E.M. Siegbahn, M.R.A. Blomberg, M.L. Blomberg, A theoretical study of the energetics of proton pumping and oxygen reduction in cytochrome oxidase, J. Phys. Chem. B 107 (2003) 10946–10955.
[16] M.R.A. Blomberg, P.E.M. Siegbahn, Quantum chemistry applied to the mechanisms of transition metal containing enzymes — cytochrome c oxidase a particularly challenging case, J. Comp. Chem. 27 (2006) 1373–1384.
[17] P.E.M. Siegbahn, M.R.A. Blomberg, Quantum chemical studies of proton-coupled electron transfer in metalloenzymes, Chem. Rev. 110 (2010) 7040–7061.
[18] D. Bloch, I. Belevich, A. Jasaitis, C. Ribacka, A. Puustinen, M.I. Verkhovsky, M. Wikström, The catalytic cycle of cytochrome c oxidase is not the sum of its two halves, Proc. Natl. Acad. Sci. U. S. A. 101 (2004) 529–533.
[19] M. Wikström, M.I. Verkhovsky, Towards the mechanism of proton pumping by the haem-copper oxidases, Biochim. Biophys. Acta 1757 (2006) 1047–1051.
[20] M. Wikström, Identification of the electron transfers in cytochrome c oxidase that are coupled to proton-pumping, Nature 338 (1989) 776–778.
[21] M.I. Verkhovsky, A. Jasaitis, M.L. Verkhovskaya, J.E. Morgan, M. Wikström, Proton translocation by cytochrome c oxidase, Nature 400 (1999) 480–483.
[22] M. Wikström, M.I. Verkhovsky, G. Hummer, Water-gated mechanism of proton translocation by cytochrome c oxidase, Biochim. Biophys. Acta 1604 (2003) 61–65.
[23] D. Jancuar, V. Berka, M. Antalik, J. Bagelova, R.B. Gennis, G. Palmer, M. Fabian, Spectral and kinetic equivalence of oxidized cytochrome c oxidase as isolated and "activated" by reoxidation, J. Biol. Chem. 281 (2006) 30319–30325.
[24] B. Kadenbach, Intrinsic and extrinsic uncoupling of oxidative phosphorylation, Biochim. Biophys. Acta 1604 (2003) 77–94.
[25] S.J. Ferguson, ATP synthase: from sequence to ring size to the P/O ratio, Proc. Natl. Acad. Sci. U. S. A. 107 (2010) 16755–16756.
[26] M. Wikström, G. Hummer, Stoichiometry of proton translocation by respiratory complex I and its mechanistic implications, Proc. Natl. Acad. Sci. U. S. A. 109 (2012) 4431–4436.
[27] P. Brzezinski, R.B. Gennis, Cytochrome c oxidase: exciting progress and remaining mysteries, J. Bioenerg. Biomembr. 40 (2008) 521–531.
[28] I. Belevich, D.A. Bloch, N. Belevich, M. Wikström, M.I. Verkhovsky, Exploring the proton pump mechanism of cytochrome c oxidase in real time, Proc. Natl. Acad. Sci. U. S. A. 104 (2007) 2685–2690.
[29] P.E.M. Siegbahn, M.R.A. Blomberg, Energy diagrams and mechanism for proton pumping in cytochrome c oxidase, Biochim. Biophys. Acta 1767 (2007) 1143–1156.
[30] P.E.M. Siegbahn, M.R.A. Blomberg, On the proton pumping mechanism in cytochrome c oxidase, J. Phys. Chem. A 112 (2008) 12772–12780.
[31] M.I. Verkhovsky, M. Wikström, Mechanism and energetics of proton translocation by the respiratory heme-copper oxidases, Biochim. Biophys. Acta 1767 (2007) 1200–1214.

[32] P. Brzezinski, P. Ädelroth, Pathways of proton transfer in cytochrome c oxidase, J. Bioenerg. Biomembr. 30 (1998) 99–107.
[33] M. Wikström, A. Jasaitis, C. Backgren, A. Puustinen, M.I. Verkhovsky, The role of the D- and K-pathways of proton transfer in the function of the haem-copper oxidases, Biochim. Biophys. Acta 1459 (2000) 514–520.
[34] K. Ganesan, R.B. Gennis, Blocking the K-pathway still allows rapid one-electron reduction of the binuclear center during the anaerobic reduction of the aa-3-type cytochrome c oxidase from *Rhodobacter sphaeroides*, Biochim. Biophys. Acta 1797 (2010) 619–624.
[35] C. von Ballmoos, R.B. Gennis, P. Ädelroth, P. Brzezinski, Kinetic design of the respiratory oxidases, Proc. Natl. Acad. Sci. U. S. A. 108 (2011) 11057–11062.
[36] H.J. Lee, J. Reimann, Y. Huang, P. Ädelroth, Functional proton transfer pathways in the heme-copper oxidase superfamily, Biochim. Biophys. Acta 1817 (2012) 537–544.
[37] P.E.M. Siegbahn, Water oxidation mechanism in photosystem II, including oxidations, proton release pathways, O-O bond formation and O_2 release, Biochim. Biophys. Acta 1827 (2013) 1003–1019.
[38] M.R.A. Blomberg, P.E.M. Siegbahn, Quantum chemistry as a tool in bioenergetics, Biochim. Biophys. Acta 1797 (2010) 129–142.
[39] P.E.M. Siegbahn, M.R.A. Blomberg, The combined picture from theory and experiments on water oxidation, oxygen reduction and proton pumping, Dalton Trans. (2009) 5832–5840.
[40] A.D. Becke, Density-functional thermochemistry. III. The role of exact exchange, J. Chem. Phys. 98 (1993) 5648–5652.
[41] M. Reiher, O. Salomon, B.A. Hess, Reparameterization of hybrid functionals based on energy differences of states of different multiplicity, Theor. Chem. Acc. 107 (2001) 48–55.
[42] Jaguar 7.6, Schrödinger, LLC, New York, NY, 2009.
[43] T. Schwabe, S. Grimme, Double-hybrid density functionals with long-range dispersion corrections: higher accuracy and extended applicability, Phys. Chem. Chem. Phys. 9 (2007) 3397–3406.
[44] P.E.M. Siegbahn, M.R.A. Blomberg, S.-L. Chen, Significant van der Waals effects in transition metal complexes, J. Chem. Theory Comput. 6 (2010) 2040–2044.
[45] M.R.A. Blomberg, P.E.M. Siegbahn, G.T. Babcock, Modeling electron transfer in biochemistry: a quantum chemical study of charge separation in *Rhodobacter sphaeroides* and photosystem II, J. Am. Chem. Soc. 120 (1998) 8812–8824.
[46] L.A. Curtiss, K. Raghavachari, R.C. Redfern, J.A. Pople, Assessment of Gaussian-3 and density functional theories for a larger experimental test set, J. Chem. Phys. 112 (2000) 7374–7383.
[47] P.E.M. Siegbahn, M.R.A. Blomberg, Density functional theory of biologically relevant metal centers, Ann. Rev. Phys. Chem. 50 (1999) 221–249.
[48] Gaussian 09, Revision C.01, Gaussian Inc., Wallingford, CT, 2010.
[49] M.R.A. Blomberg, P.E.M. Siegbahn, Why is the reduction of NO in cytochrome c dependent nitric oxide reductase (cNOR) not electrogenic? Biochim. Biophys. Acta 1827 (2013) 826–833.
[50] M.R.A. Blomberg, P.E.M. Siegbahn, Mechanism for N_2O generation in bacterial nitric oxide reductase: a quantum chemical study, Biochemistry 51 (2012) 5173–5186.
[51] P.E.M. Siegbahn, M.R.A. Blomberg, Modeling of mechanisms for metalloenzymes where protons and electrons enter or leave, in: K. Morokuma, J. Musaev (Eds.), Computational Modeling for Homogeneous Catalysis and Biocatalysis, Wiley-VCH, Germany, 2008, pp. 57–81.
[52] M. Karpefors, P. Ädelroth, A. Namslauer, Y. Zhen, P. Brzezinski, Formation of the "peroxy" intermediate in cytochrome c oxidase is associated with internal proton/hydrogen transfer, Biochemistry 39 (2000) 14664–14669.
[53] V.R.I. Kaila, M.I. Verkhovsky, G. Hummer, M. Wikström, Mechanism and energetics by which glutamic acid 242 prevents leaks in cytochrome c oxidases, Biochim. Biophys. Acta 1787 (2009) 1205–1214.
[54] M.R.A. Blomberg, P.E.M. Siegbahn, A quantum chemical study of the mechanism for proton coupled electron transfer leading to proton pumping in cytochrome c oxidase, Mol. Phys. 108 (2010) 2733–2743.
[55] I.A. Sirnova, P. Ädelroth, R.B. Gennis, P. Brzezinski, Aspartate-132 in cytochrome c oxidase from *Rhodobacter sphaeroides* is involved in a two-step proton transfer during oxo-feryl formation, Biochemistry 38 (1999) 6826–6833.
[56] V. Rauhamäki, D.A. Bloch, M. Wikström, Mechanistic stoichiometry of proton translocation by cytochrome cbb-3, Proc. Natl. Acad. Sci. U. S. A. 109 (2012) 7286–7291.
[57] R. Murali, G. Gökce, F. Daldal, R.B. Gennis, Stoichiometry of proton pumping by the cbb-3 oxygen reductase in whole cells of *Rhodobacter capsulatus* at pH 7 is about $0.5H^+$ per electron, Proc. Natl. Acad. Sci. U. S. A. (2012) E2144.
[58] V. Rauhamäki, D.A. Bloch, M. Wikström, Reply to Murali, et al., Proton translocation stoichiometry of cbb-3-type cytochrome c oxidase, Proc. Natl. Acad. Sci. U. S. A. (2012) E2145.